



Shear Rates in Mixing of Viscoelastic Fluids by Helical Ribbon Impeller

Mansour Jahangiri

Department of Chemical Engineering, Semnan University, Semnan-19919, Iran

Received 17 May 2008; accepted 22 November 2008

ABSTRACT

One of the basic problems in the mixing of non-Newtonian fluids and especially diluted polymer solutions is the determination of the prevailing shear rates during the mixing process. The significant method of Metzner and Otto for calculation of the effective shear rate is limited to the laminar region and it is not valid in the transition region. In this article, the local shear rate and the Metzner-Otto method for helical ribbon impeller have been studied using laser Doppler anemometry (LDA) for viscoelastic liquids. It is also shown that the variation of the local shear rate against the impeller speed is better correlated by a power equation, i.e., $\dot{\gamma} = k'_s \cdot N^b$ in the transition region, i.e., $70 < Re < 6700$. In addition, a correlation between the improved coefficient, k'_s , and the elasticity number of the viscoelastic liquid is given that can be helpful in designing the mixing of viscoelastic as well as inelastic non-Newtonian fluids by means of relating the rheological properties to the kinematical and dynamical parameters of the mixing process.

Key Words:

LDA;
helical ribbon impeller;
viscoelastic liquids;
mixing.

INTRODUCTION

In many branches of polymerization process, chemical industry, biotechnology, and environmental technology, stirred tank reactors are important components of the processing plants [1]. Helical ribbon impellers are capable of producing vertical circulation patterns (axial pumping) over the entire

vessel volume and they have a rather good homogenization potential for mixing of viscous Newtonian and non-Newtonian liquids [1,2]. Additional difficulties for optimization of the process often occur with the latter fluids. In fact, the hydrodynamics strongly depends on the nature of the fluids

(*) To whom correspondence to be addressed.
E-mail: M_Jahan98@yahoo.com

involved in the mixing system. Non-Newtonian inelastic fluids and principally viscoelastic fluids are still poorly understood in this respect. For these specific reasons numerical and analytical studies are appropriate means to obtain information about both hydrodynamics and the nature of fluids in the mixing process [3]. Mixing of low viscosity liquids is usually achieved in turbulent flow to take advantages of the rapid mixing. However, for many industrial materials, such as viscoelastic polymeric liquids, suspensions, it is impossible or impractical to operate under turbulent mixing. It might proceed in the laminar or at best in the transition flow mixing regime. Available data for the laminar region have been used to design and scale up mixing operations in the transition region due to the lack of information in this region [4]. Due to complexities and uncertainties of mixing in the transition region, it makes difficult to predict mixing performance for rheological complex non-Newtonian fluids especially for scale up [5]. Most previous works are limited to the laminar flow region [1,2,4,5]. Only a few works on the mixing of viscoelastic liquids with helical ribbon impellers in the transition region are available in the literature [4,5]. Investigation of the detailed velocity profiles and local shear rates will provide the most useful information for analyzing the performance of the impeller. The influence of viscoelasticity on the flow pattern is complex. The complexity is essentially due to the complicated shape of agitator, non-linear terms in the rheological equation of state as well as non-linear inertial terms in the equation of motion [5-7].

The anisotropic character of viscoelastic properties is a feature of many directed polymer systems [8]. For most non-Newtonian fluids, a non-trivial scaling theory is not possible [9,10].

The classical approach to estimate the shear rate in stirred tanks is the use of the Metzner-Otto method [11]. Accordingly, a given impeller rotational speed, N , produces an effective rate of deformation, $\dot{\gamma}_e$, in the mixing vessel which could be estimated by:

$$\dot{\gamma}_e = k_s \cdot N \quad (1)$$

where N is the rotational speed of the impeller in round per second (rps) and k_s is the Metzner-Otto coefficient. It is a constant of proportionality which

must be evaluated experimentally for each mixing system. The value of k_s in eqn (1) is estimated by using power consumption measurement for Newtonian and non-Newtonian fluids using identical impeller rotational speed and the same mixing system arrangement [9]. Although originally the constant k_s was postulated to be a true constant for a given mixing system geometry and independent of liquid rheology, but subsequently it has been found to be function of power law index thereby suggesting the effective shear rate to be function of the rheological properties of the mixing liquid. However, for helical ribbon impeller considerable confusion exists in the literature regarding the dependence of the constant k_s on the fluid property [10]. Various numerical analyses have confirmed or extended the validity of eqn (1) [12-15]. However, the significance of the Metzner-Otto method to calculate the effective deformation rate is limited to the laminar flow region and is not valid in the transition region [1,7,15]. Ulbrecht et al. [5] pointed out that the use of the Metzner-Otto method could lead to very large errors for scale up in the transition region ($Re > 10$). It is worth noting that although most laboratory-scale tests are carried out in the laminar flow region, the scale up usually results in a change to a transitional or turbulent region. A failure in the prediction of this transition can result in a misapplication of the Metzner-Otto method. It is suggested that viscoelastic effects are expected to become less significant on scale up. This is because the Deborah number, which is the ratio of the fluid relaxation time to the process time, generally decreases on scale-up due to the increased process time. For example, the process time, $1/N$, is of the order for the case of constant tip speed and of the order of $D^{2/3}$ for the case of constant power per unit volume [14]. Forschner et al. [15] mentioned that the Metzner-Otto method overestimates the power input for non-Newtonian fluids in the transition region. This is due to the additional shear caused by increasing velocity fluctuations. Cheng et al. [4] had extensive study on the effects of the non-Newtonian and viscoelastic properties on the effective rate of deformation in the transition region. They proposed three different models based on the equivalent Couette flow and showed that the effective rate of deformation increased with the impeller rotational speed in the transition region. The experiments per-

formed by Carreau et al. [7] showed that the fluid elasticity tends to decrease the effective rate of deformation in the transition region. However, the majority of the published investigations on the shear rate for helical ribbon impellers are concerned with the calculation of the average shear rate of non-Newtonian fluids in mixing vessels [1,4,7,14,15].

The local energy dissipation can be written in terms of mean and fluctuation components of these velocities as:

$$\dot{\varepsilon} = (\rho / \mu) [d(U + u') / dx]^2 \quad (2a)$$

where $\dot{\varepsilon}$, ρ , μ , U , and u' are dissipation energy rate, density, viscosity of bulk fluid, average velocity, and fluctuation velocity, respectively. Eqn (2a) implies that the shear rate is proportional to the square root of the local dissipation energy (or power per unit mass) in fully turbulent region. This equation has been confirmed experimentally by Wichterle et al. [16] who used an electrochemical method to measure the shear rate on the Rushton turbine impeller blade. Their correlation for the shear rate is:

$$\dot{\gamma} = (1 + 5.3)^{1/n} Re^{1/(n+1)} N \quad (2b)$$

In which, $\dot{\gamma}$, n , Re , and N are shear rate, power law index, Reynolds number, and rotational speed, respectively. This equation may be written for a Newtonian fluids ($n=1$) as:

$$\dot{\gamma} \approx (N^3 D^2)^{0.5} \approx (\dot{\varepsilon})^{0.5} \quad (2c)$$

which is expected theoretically. Höcker et al. [17] and Bourne et al. [18] have also proposed expressions which relate the shear rate in the transitional or turbulent fluid to the power input. These results are important in the design of shear sensitive mixing systems since the contribution of turbulence to shear is at least one order of magnitude greater than the contribution from velocity profile. Therefore, estimating the shear rate in turbulent flow based on Metzner-Otto method will seriously underestimate its true value [19]. It becomes very important to know which shear rate is used to calculate the effective viscosity for non-Newtonian fluids. Blending time and heat transfer in agitated vessel are very important in mixing vessels.

For turbine system Metzner-Otto concept does not work well for heat transfer at a wall and for blending durations. In these cases the local shear rate is much lower than around the impeller defined by eqn (1). Thus the local viscosity is much higher with corresponding longer blend times and lower heat transfer coefficients. In the transition and turbulent region this equation works poorly because the local shear rates are higher than the viscous shear rates predicted near the impeller by this equation. For viscoelastic liquids the role of viscoelasticity appears to be ambiguous [5,14,15]. As far as I am aware, no prior results about local shear rate of impeller on the mixing of viscoelastic liquids based on LDA velocity measurements are available in the literature [1-3,9,20]. The originality and novelty of this work is to investigate local shear rate values of helical ribbon impeller and correlate them with viscoelastic liquid properties and flow regime in the mixing tank. The objective of this work is two folds: (i) to obtain the local shear rate of helical ribbon impeller in mixing viscoelastic liquids directly from LDA velocity measurements in the transition region, (ii) to investigate the possibility of applying an appropriate correlation between local shear rate and impeller rotational speed. Also, efforts have been made to establish a relationship between the improved coefficient, k'_s , and the elasticity of poly(acrylamide) (PAA) solutions at this work. Corresponding values of the viscosity and the dimensionless group such as the elasticity and Weissenberg numbers that characterize the fluid under consideration are calculated in terms of the local shear rate or the improved coefficient, k'_s .

EXPERIMENTAL

Method

Mixing experiments were performed in a cylindrical plexiglas tank with an inside diameter of $D = 276$ mm and a wall thickness of 3 mm. The height of the liquid in the tank was kept at 210 mm. The LDA system (Dantec Measurement Technology) consisted of a 5 W Spectra-Physics argon-ion laser, two-colour modular optics, two Burst Spectrum Analyzers and a PC. The front focusing lens had a focal length of 310 mm and produced a beam angle of 9.92° . The

power of the emitted blue-green beam could be regulated up to 5 W. This beam was split by a modular optical system into four beams in such a way that two of them were blue rays having a wavelength of 488.0 nm and two others were green with a wavelength of 514.5 nm. The LDA system was operated in the backscatter mode, with both receiving and transmitting optics in the same module. The total number of the collected bursts at each point was such that for any larger number of bursts, only the variations less than 10 mm/s in the velocity could be sensed. An oversize filter accepted only the signals from the smallest particles. Calculated average values could be biased in such flows. Poly(acrylamide) LT27 from Magnofloc UK was dissolved in 50 wt% glycerin-water mixtures at four concentrations of 500, 900, 1100, and 1350 ppm. The fluids were denoted as A, B, C, and D, respectively. More detailed descriptions of the experimental setup and procedure are available elsewhere [21]. Also, rheological behaviours of the test fluids were discussed in this reference.

Dimensionless Numbers

It has been shown that the key dimensionless group for the reversal flow pattern in the mixing of viscoelastic fluids is the elasticity number defined as follows [22]:

$$El = \frac{Wi}{Re} \quad (3a)$$

where the Weissenberg and Reynolds numbers are defined as:

$$Wi = \frac{N_1}{\tau_{12}} = \lambda_0 \dot{\gamma}_{tip} \quad (3b)$$

$$Re = \frac{\rho ND^2}{\eta_0} \quad (3c)$$

In which ρ , D , η_0 , λ_0 , and $\dot{\gamma}_{tip}$ denote the fluid density, the impeller diameter, zero shear rate viscosity, Maxwell relaxation time and shear rate at the impeller tip; the latter will be explained later in detail. N_1 and τ_{12} represent the first normal stress difference and the shear stress in the steady shear condition, which are determined using the upper convected Maxwell model [21,23-26]. It is worth noticed that the shear rates at the impeller tip are calculated

from modified Metzner-Otto correlation in this work,

$$\dot{\gamma}_{tip} = k'_s \cdot N^{b'} \quad (3d)$$

where N , k'_s , and b' are the rotational speed of the impeller in round per second (round/s), improved coefficient and a constant parameter, respectively, introduced in this work, i.e., eqn (6).

RESULTS AND DISCUSSION

In order to measure the local velocity components in the mixing of the PAA solutions, at a vertical location of $z/H = 0.57$, twenty-five radial positions away from the impeller shaft to the vessel wall were chosen where z and H denote the vertical coordinate and the height of the tanks, respectively. The points were equally spaced such that r_i in mm equaled $10+5(i-1)$ for $i = 1, 2, \dots, 25$. The origin of the coordinate system used, was the centre of the vessel base plate. The local velocities at these points were measured at the impeller rotational speeds corresponding to the transition region of $70 < Re < 6700$. To find suitable correlations for the profiles of local tangential velocity, V_t / V_{tip} , at the front face of the impeller blade in the transition region, several relationships were examined following the works of Cheng et al. [4] and Carreau et al. [27]. It was concluded that these velocity profiles could be obtained satisfactorily through the consideration of two zones instead of one. The first zone relied between the impeller shaft and the impeller blade Z1-Z2. The second one was related to the neighbourhood of the impeller blade at the front face Z2-Z3-Z4-Z5 in Figure 1. It was shown that the following equation fairly correlated the local tangential velocity with the impeller speed for PAA solutions in the transition region $70 < Re < 6700$ [21]:

$$V_t / V_{tip} = m_0 + n_0 (r / R) \quad (4)$$

where m_0 and n_0 are functions of Reynolds and elasticity numbers. In these equations, the ranges of N and El are $0.42 < N < 1.67$ round/s and $0.07 < El < 0.11$, respectively.

Figure 1 is a typical comparison between the correlation results of eqn (4) and the experimental data

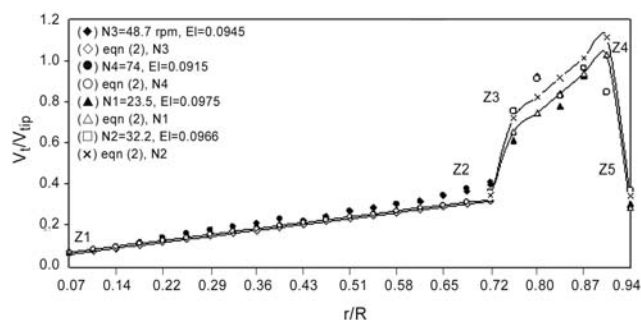


Figure 1. Predicted values of eqn (4) for tangential velocity of helical ribbon impeller in mixing of PAA solutions.

for 1350 ppm PAA solution (fluid D) at different impeller speeds. This figure showed that the linear correlations such as those proposed here were suitable relationships for correlating V_t/V_{tip} data in the transition region. More information is given in the references [21-26].

Shear Rate

The fluid motion caused by the rotating helical ribbon impeller is approximated by an equivalent flow produced in a coaxial cylinder system with the inner cylinder rotating [7]. For a steady and fully developed Couette flow, neglecting the end effects, we can write [28]:

$$\dot{\gamma}_{tr} = -r \frac{\partial(v_t / r)}{\partial r} \tag{5a}$$

The fluid experiences a nearly rigid body motion in the region between the impeller shaft and the inside of the impeller blade, i.e., Z1-Z2 region in Figure 1. Therefore, the shear rate is nearly negligible in this region. For the regions of considerable shear deformation rates near the inside and outside of the impeller blade a discrete version of the above equation was employed reading as:

$$(\dot{\gamma}_{tr})_{r_i} = -r_i \frac{\left. \frac{v_t}{r} \right|_{r=r_{i+1}} - \left. \frac{v_t}{r} \right|_{r=r_i}}{r_{i+1} - r_i} \quad i = 19, 20, \dots, 24 \tag{5b}$$

where $r = r_{19} = 100$ mm and $r = r_{24} = 125$ mm correspond to the inside and outside of the impeller blade, respectively. An example of the shear rate profiles for 1350 ppm PAA solution is shown in Figure 2.

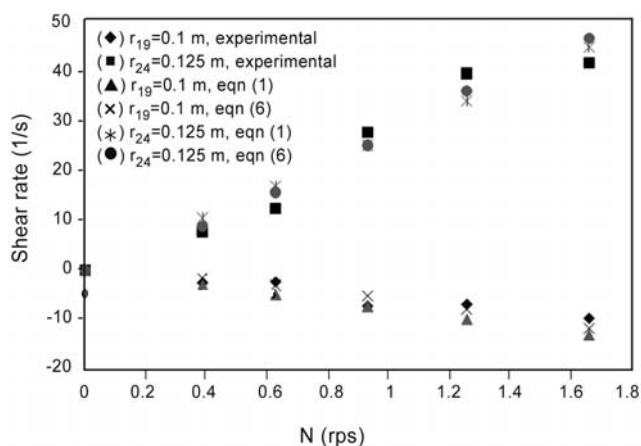


Figure 2. A comparison of eqns (1) and (6) and experimental data for 1350 ppm PAA solutions.

The shear rate increases with impeller speed nearly in a power law relationship in the gap, i.e., $r > r_{24}$, between the impeller blade and vessel wall. Also, the most variations of shear rates occur in the neighbourhood of the impeller blade, particularly at inner and outer tip of the impeller. Figure 2 indicates that shear rate has a steep increase in the range of $N > 0.6$ rps. Because of the centrifugal forces generated by the tangential flow, a secondary flow is created heading away from the impeller towards the vessel wall. The opposite direction of tangential velocities caused to have negative values of shear rates as going from the shaft to the vicinity of the impeller blade because of axial pumping action of the helical ribbon impeller [5,28].

Modified Metzner-Otto Equation

Based on the Metzner and Otto concept [11], the following equation is proposed for correlating the local shear rates of helical ribbon impellers in the transition region:

$$\dot{\gamma} = -r \partial(v_t / r) / \partial r = k'_s \cdot N^{b'} \tag{6}$$

Figure 2 gives a comparison for local shear rates between eqns (1) and (6) and experimental data of 1350 ppm polyacrylamide (PAA) solution. This figure reveals that eqn (6) has well predicted shear rate data of this work. Also, mean relative errors of eqns (1) and (6) are 21 and 13 percent, respectively. Also,

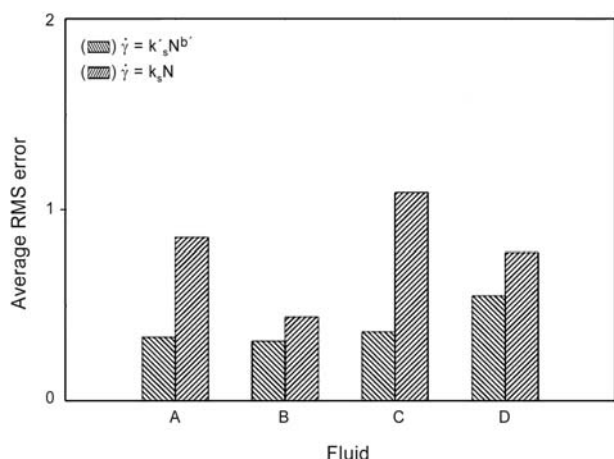


Figure 3. Average RMS errors of eqns (1) and (6) for different PAA solutions.

in order to assess the data fitting ability of eqns (1) and (6), it may be used root mean square (RMS) error analysis [29].

An RMS-error analysis was carried out to assess the data fitting ability of eqns (1) and (6) using the local relative error, ε_i , where the RMS error is defined as:

$$RMS\ Error = \sqrt{\frac{\sum_i \varepsilon_i^2}{N_D}} \quad (7)$$

in which N_D is the total number of data points. An example of the average RMS error for eqns (1) and (6) is displayed in Figure 3. As the figure shows clearly, the average RMS error of eqn (1) for different PAA solutions is larger than that of eqn (6) in all cases. It can also be seen that the average error associated with eqn (6) has a nearly monotonous trend with the concentration of the PAA solution while that of eqn (1) is randomly variable with the solution concentration. However, we note that the smaller error and a well-defined trend for the errors of eqn (6) are attributed to the presence of an extra parameter, b' . Thus, we conclude that eqn (6) is more suitable for the calculation of shear rate data of Figure 2 especially in the gap between the impeller blade and the vessel wall.

Determination of k'_s and k_s

One of the aims of this work is to investigate local shear rate values of helical ribbon impeller and corre-

late them with viscoelastic liquid properties and flow regime in the mixing tank. Therefore, eqns (6) and (8b) are introduced in this work. Also, It may be revealed that no prior results about local shear rate of helical impeller on the mixing of viscoelastic liquids based on LDA velocity measurements are available in the literature [1,2,21,33]. Therefore, it may not have any parameter to join to the literature and making comparison to the results of this work. One of the goals of this work is introducing improved coefficient, k'_s , instead of Metzner-Otto coefficient, k_s . Because improved coefficient, k'_s , is a new parameter and it is not available in literature, then it may be necessary to use Metzner-Otto coefficient, k_s , in order to make a comparison with literature. Also, method of obtaining k_s and k'_s in this work is fully different from literature. In other words, the Metzner-Otto coefficient, k_s , in this work is directly calculated from local shear rate based on LDA velocity measurements with high accuracy. However, the Metzner-Otto coefficient, k_s , in the literature may be obtained indirectly such as power consumption or electrochemical methods [14,16,20]. Table 1 shows that k_s which was calculated directly from local shear rate in this work was consistent with literature. This may be sure to have confidence in k'_s calculations. Therefore, in this work, the use of local shear rate and k'_s are encouraged to using in design purposes in mixing of viscoelastic liquids with helical ribbon impeller in the transition region.

In order to determine the local values k_s , k'_s and b' , shear rate data of Figure 2 for PAA solutions and eqns (1), (5b) and (6) were used. Variations of k_s and k'_s in eqns (1) and (6) for helical ribbon impeller for different PAA solutions are shown in Figure 4. This figure shows that the maximum values of k_s and k'_s belong to the impeller blade tip in the gap between the impeller blade and vessel walls, $r/R \geq 0.72$ and these values are less than 5 in the central core between the shaft and blade of the impeller, $r/R < 0.72$. Figure 4 shows that k_s and k'_s values are not constant with respect to radial positions and vary with the radius of mixing vessel. Mean relative error between k_s and k'_s in Z1-Z2 region of Figure 1 is about 18.5 percent and in Z2 to Z5 region is nearly 35 percent. Therefore, it was not possible to consider that the value of k_s is the same as k'_s . Also, as revealed from this figure, the

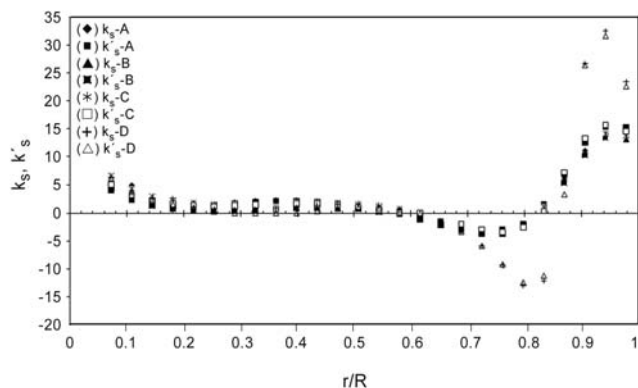


Figure 4. Variations of k_s and k'_s in eqns (1) and (6) for helical ribbon impeller for different PAA solutions.

values of k_s are small for PAA solutions [21], with respect to non-Newtonian inelastic fluids [30] being in agreement with the work of Ducla et al. [31] and Nienow et al. [32].

In addition, some comparisons of several k_s values for helical ribbon impellers obtained or used by a number of authors is given in Table 1. This table reveals that indeed some values of k_s in literature are different from each other due to various parameters such as flow regime, fluid property and mixing system specifications [5,9,14,33]. As a first approximation, it is enough to calculate k'_s (or k_s) at the inner and outer impeller tips from the local shear rate data of Figure 2 based on the LDA technique. The value of k_s in this work is close to values given in literature [9,30,34]. The effect of flow regime on k_s is one reason for using k'_s (in eqn (6)) as discussed by Carreau et al. [7] and Cheng et al. [4]. Thus the use of the improved correlation, eqn (6), instead of the Metzner and Otto relationship, eqn (1), could not lead to erroneous results and inadequate designs and this is in agreement with literature [4,5,7]. Values of b' in Z1-Z5 region can be taken as the local value at the

Table 1. Values of k_s from literature for typical helical ribbon impellers.

Researcher	T/D	n	Re	k_s
Bourne et al. [41]	1.1	0.4-1	$N^{2-n}D^2 \rho/k$	66.06
Hall et al. [35]	1.1-1.11	0.35-1	$\rho ND^2 / \mu_0$	27
Rieger et al. [36]	1.053	0.5-1	$N^{2-n}D^2 \rho/k$	36.73
Nagata [37]	1.056	0.27-1	$\rho ND^2 / \mu_0$	30
Yap et al. [38]		0.27		16.2-24.2
Yap et al. [38]	1.135	0.17-0.65	$\rho ND^2 / \eta_e$	79.85
Shamlou et al. [40]	1.1	-	$\rho ND^2 / \mu$	26.8
Kuriyama et al. [39]	1.05-1.163	0.35-0.75		24.68
Carreau et al. [7]	1.110	0.183-1	$\rho ND^2 / \eta_e$	17-40
Cheng et al. [4]	1.693	0.122-1	$\rho ND^2 / \eta_e$	16
Cheng et al. [43]		0.33		20.5-28
Brito-De la Fuente et al. [44]		0.14-0.36		7.5-26.6
Brito-De la Fuente et al. [30]	1.135	0.133-1	$N^{2-n}D^2 \rho/k$	5-32.9
Brito-De la Fuente et al. [34]	1.17	0.22±0.02	$\rho ND^2 / \eta$	10-30
Shekhar et al. [20]		0.3-1.0		21.7
Delaplace et al. [9]		$n < 1$	$\rho ND^2 / \mu$	10-35
Montante et al. [42]	0.43	0.68	$\rho ND^2 / \mu_0$	11
The work (outer impeller blade tip)	1.08	‡	$\rho ND^2 / \eta_0$	33

‡ See ref. [21] for the model and parameters.

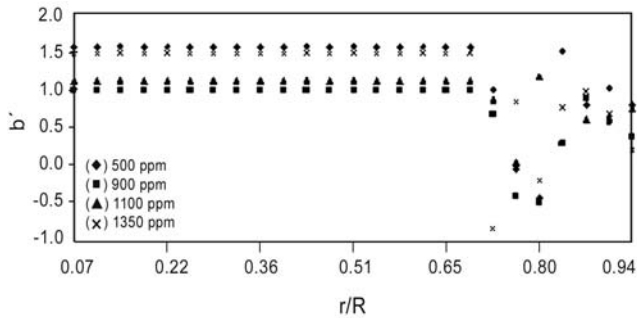


Figure 5. Variation of b' (in eqn (6)) for various concentrations of PAA solutions.

vicinity of inner and outer impeller tip for using in eqn (6). Variations of b' in the improved correlation, eqn (6), for different concentrations of PAA the solutions are shown in Figure 5. This figure shows that the value of b' does not change considerably except for high concentrations of PAA solutions in Z1-Z2 region of Figure 1. Also it is concluded that, in this region although b' is not equal to 1.0 as in eqn (1), it is possible to consider a constant value for it except for one concentration. This was not done here and changes in b' in whole region of tank were allowed.

Elastic Effects

The values of elasticity number depend on the liquid elasticity and the impeller type [22,24,25]. Although the concentration of polymer additives is small, (say less than 1000 ppm, [21]), the elastic behaviour might still be quite significant in the transition or turbulent

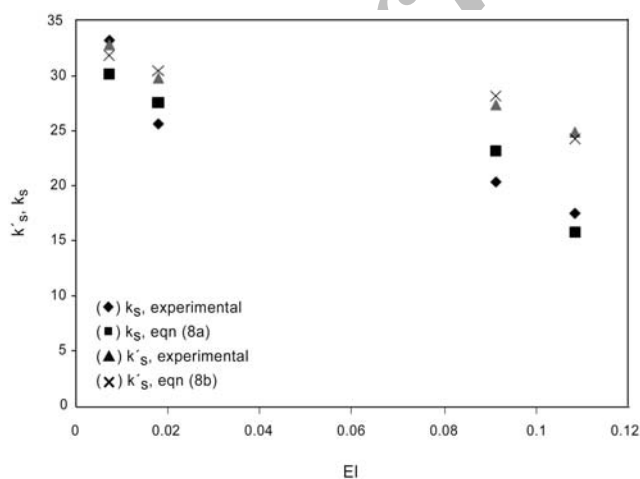


Figure 6. Predicted values of k_s and k'_s by eqns (8a) and (8b).

Table 2. Experimental values of k_s and k'_s .

El	k_s	k'_s
0.0075	33.1367	32.78
0.018106	25.584	29.74
0.0912	20.34	27.30
0.1083	17.506	24.821

regime [5]. The modified upper convected Maxwell model [21,23-25] may be used for determining the relationship between k'_s and the fluid elasticity. Zero shear rate viscosity and Maxwell relaxation time can be calculated by using the modified upper convected Maxwell model. The elasticity number can be determined using eqn (3a). The result in Figure 6 shows that the values of k'_s decrease with the elasticity number which is consistent with literature [30-32]. In order to establish the effect of all rheological parameters on the improved coefficient in the transition region, data of this work have been analyzed to obtain the correlation between the values of k_s and k'_s (Table 2) in the vicinity of outer impeller blade and the elasticity number as the following equations:

$$k_s = 31.18 - 125.15 El \quad (8a)$$

$$k'_s = 32.2 - 63.048 El \quad (8b)$$

Eqn (8b) may be used to estimate k'_s for dilute viscoelastic solutions by knowing the elasticity number in the range of $0.007 < El < 0.11$ that takes place in the transition region. The mean deviation of eqn (8b) is about 3.2 percent. Also, this equation can be used to estimate the variation of maximum shear rate and power consumption of viscoelastic fluids in mixing processes in the transition region.

CONCLUSION

LDA velocity measurements in different concentrations of polyacrylamide (PAA) solutions for a helical ribbon impeller have produced results in the transition region, i.e., $70 < Re < 6700$ as follows:

1. The dimensionless local tangential velocity distributions were reasonably correlated with consid-

ering two regions using linear correlation.

2. Local fluid shear rates are not directly proportional to rotational impeller speed in the agitation of PAA solutions in the transition region.

3. The correlation between variation of local shear rate and corresponding rotational impeller speed may be well expressed through a power-law relationship.

4. A given correlation in this work, between k'_s and elasticity number El , can be used for design purposes for mixing of PAA solutions in agitated vessels.

NOTATIONS

a, b, b', c, d	Constants
D	Impeller diameter (m)
H	Height of liquid in agitated vessel
d	Stretch tensor ($d = 1/2 (\nabla v + (\nabla v)^\dagger)$)
El	Elasticity number
k_s	Metzner-Otto coefficient
k'_s	Improved coefficient
n	Power law index
N	Rotational speed (round/s)
N_D	Number of data points
N_1	First normal stress difference (Pa)
r	Radial coordinate (m)
R	Radius of agitated vessel (m)
Re	Reynolds number ($\rho ND^2/\eta_0$)
SD	Standard deviation
T	Agitated vessel diameter (m)
U	Average velocity (m/s)
u'	Fluctuation velocity (m/s)
∇v	Velocity gradient
v_r	Radial velocity (m/s)
v_t	Tangential velocity (m/s)
V_{tip}	Impeller blade tip speed (m/s)
z	Axial coordinate (m)
Wi	Weissenberg number

Greek symbols

$\dot{\gamma}$	Shear rate (1/s)
$\dot{\gamma}_e$	Effective shear rate (1/s)
$\dot{\gamma}_{tip}$	Impeller tip shear rate (1/s)
$\dot{\epsilon}$	Dissipation energy rate (W)
ϵ_i	Local relative error ($(f_{i,exp} - f_{i,pred})/f_{i,exp}$)
μ	Viscosity of bulk fluid (kg/ms)
η_0	Zero shear rate viscosity (kg/ms)

λ_0	Zero shear rate Maxwell relaxation time (s)
τ_{12}	Shear stress (Pa)
ρ	Fluid density (kg/m ³)
ω	Angular frequency of oscillatory shear flow (rad/s)
Π_d	Second invariant of the strain tensor

Superscripts

'	Fluctuating values
†	Transpose of a second order tensor

Subscripts

pred	Predicted values proposed by correlations
exp	Experimental data
r,t	Radial and tangential components

REFERENCES

1. Foucault S, Gabriel A, Tanguy PA, Power characteristics in coaxial mixing: Newtonian and non-Newtonian fluids, *Ind Eng Chem Res*, **44**, 5036-5043, 2005.
2. Takahashi K, Horiguchi H, Mishima M, Yatomi R, Mixing characteristics in a vessel agitated by large paddle impeller maxblend, *12th Eur Conf on Mixing, Bologna*, 27-30 June, 2006.
3. Ein-Mozaffari F, Bennington CPG, Dumont GA, Suspension yield stress and the dynamic response of agitated pulp chests, *Chem Eng Sci*, **60**, 2399-2408, 2005.
4. Cheng J, Carreau PJ, Mixing in the transition flow regime with helical ribbon agitators, *Can J Chem Eng*, **72**, 418-430, 1994.
5. Ulbrecht JJ, Carreau PJ, Mixing of viscous non-Newtonian liquids in "mixing of liquids by mechanical agitation," Ulbrecht JJ, Patterson GK (Eds), *Gordon and Breach Science, New York*, 1985.
6. Ann-Archard DL, Boisson HC, A finite element simulation of the crossed-effects of viscoelasticity and inertia in an agitated vessel, *Int J Numer Meth Fluids*, **21**, 75-90, 1995.
7. Carreau PJ, Chhabra RP, Cheng J, Effect of rheological properties on power consumption with

- helical ribbon agitators, *AIChE J*, **39**, 1421-1430, 1993.
8. Volkov VS, Spectral decomposition in anisotropic liquids, *Electronic-Liquid Crystal Communications*, 2008 (http://www.e-lc.org/docs/2008_02_15_05_42_26).
 9. Delaplace G, Guerin R, Leuliet JC, Chhabra RP, An analytical model for the prediction of power consumption for shear-thinning fluids with helical ribbon and helical screw ribbon impellers, *Chem Eng Sci*, **61**, 3250-3259, 2006.
 10. Chhabra RP, Fluid mechanics and heat transfer with non-Newtonian liquids in mechanically agitated vessels, *Adv Heat Trans*, **37**, 77-178, 2003.
 11. Metzner AB, Otto RE, Agitation of non-Newtonian fluid, *AIChE J*, **3**, 3-10, 1957.
 12. Metzner AB, Taylor JS, Flow patterns in agitated vessels, *AIChE J*, **6**, 109-114, 1960.
 13. Hiraoka S, Yamada I, Mizoguchi K, Two dimensional model analyses of flow behavior of highly viscous non-Newtonian fluid in agitated vessel with paddle impeller, *J Chem Eng Japan*, **12**, 56-62, 1979.
 14. Doraiswamy D, Grenville RK, Etchells AW, Two score years of the Metzner-Otto correlation, *Ind Eng Chem Res*, **33**, 2253-2258, 1994.
 15. Forschner P, Krebs R, Schneider T, Scale-up procedures for power consumption of mixing in non-Newtonian fluids, *Proc 7th Eur Conf on Mixing, Brugge, Belgium*, 161, 1991.
 16. Wichterle K, Kadlec M, Zak L, Mitschka P, Shear rates on turbine impeller blade, *Chem Eng Commun*, **32**, 289-305, 1985.
 17. Höcker H, Langer G, Werner U, Power consumption of stirrers in non-Newtonian liquids, *Ger Chem Eng*, **4**, 113-123, 1981.
 18. Bourne JR, Buerli M, Regenass W, Power and heat transfer to agitated suspensions: use of heat flow calorimetry, *Chem Eng Sci*, **36**, 784-787, 1981.
 19. Bowen R, Unravelling the mysteries of shear sensitive mixing systems, *Chem Eng*, **9**, 55-63, 1986.
 20. Shekhar SM, Jayanti S, Mixing of pseudoplastic fluids using helical ribbon impellers, *AIChE J*, **49**, 2768-2772, 2003.
 21. Jahangiri M, Velocity distribution of helical ribbon impeller in mixing of polymeric liquids in the transition region, *Iran Polym J*, **16**, 731-739, 2007.
 22. Ulbrecht J, Mixing of viscoelastic fluids by mechanical agitation, *Chem Eng (London)*, **286**, 347-353, 1974.
 23. Narenji MRG, Free Coating of Viscoelastic Fluids, *PhD Thesis, Univ of Bradford, UK*, 1978.
 24. Jahangiri M, Narenji MRG, Montazerin N, Savarmand S, Investigation of the viscoelastic effect on the Metzner and Otto coefficient through LDA velocity measurements, *Chin J Chem Eng*, **9**, 77-83, 2001.
 25. Savarmand S, Narenji MRG, Wilkinson WL, Modifications to non-linear rheological models of viscoelastic fluids, *Iran Polym J*, **7**, 195-203, 1998.
 26. Jahangiri M, Fluctuation velocity for non-Newtonian liquids in mixing tank by Rushton turbine in the transition region, *Iran Polym J*, **15**, 285-290, 2006.
 27. Carreau PJ, Patterson I, Yap CY, Mixing of viscoelastic fluids with helical-ribbon agitators: I. Mixing time and flow patterns, *Can J Chem Eng*, **54**, 135-142, 1976.
 28. Bird RB, Armstrong RC, Hassager O, *Dynamics of Polymeric Liquids, Fluid Mechanics*, 2nd ed, Vol. 1, John Wiley, New York, 1987.
 29. Cramer SD, Marchello JM, Numerical evaluation of models describing non-Newtonian behaviour, *AIChE J*, **14**, 980-982, 1968.
 30. Brito-De La Fuente E, Choplin L, Tanguy PA, Mixing with helical ribbon impellers: effect of highly shear thinning behavior and impeller geometry, *Trans IChem E*, **75**, 45-52, 1997a.
 31. Ducla JM, Desplanches H, Chevalier JL, Effective viscosity of non-Newtonian fluids in a mechanically stirred tank, *Chem Eng Commun*, **21**, 29-36, 1983.
 32. Nienow AW, Elson TP, Aspects of mixing in rheologically complex fluids, *Chem Eng Res Des*, **66**, 5-15, 1988.
 33. Anne-Archard D, Marouche M, Boisson HC, Hydrodynamics and Metzner-Otto correlation in stirred vessels for yield stress fluids, *Chem Eng J*, **125**, 15-24, 2006.
 34. Brito-De La Fuente E, Nunez MC, Tanguy PA,

- "Non-isothermal mixing of rheologically complex fluids with close-clearance impellers. Effect of natural convection", *Chem Eng Tech*, **20**, 203-207, 1997.
35. Hall KR, Godfrey JC, Power consumption by helical ribbon impellers, *Trans Chem E*, **48**, T201-T209, 1970.
 36. Rieger F, Novak V, Power consumption of agitators in highly viscous non-Newtonian liquids, *Trans I Chem E*, **51**, 105-111, 1973.
 37. Nagata S, *Mixing: Principles and Applications*, Kodansha Ltd. and John Wiley, New York, 1975.
 38. Yap CY, Patterson WI, Carreau PJ, Mixing with helical ribbon agitators, *AIChE J*, **25**, 516-521, 1979.
 39. Kuriyama M, Arai K, Saito S, Mechanism of heat transfer to pseudoplastic fluids in an agitated tank with helical ribbon impeller, *J Chem Eng Japan*, **16**, 489-494, 1983.
 40. Shamlou PA, Edwards MF, Power consumption of helical ribbon mixers in viscous Newtonian and non-Newtonian fluids, *Chem Eng Sci*, **40**, 1773-1781, 1985.
 41. Bourne JR, Butler H, Power consumption of helical ribbon impellers in viscous liquids, *Trans IChem E*, **47**, T263-T270, 1969.
 42. Montane G, Mostek M, Jahoda M, Magelli F, CFD simulations and experimental validation of homogenisation curves and mixing time in stirred Newtonian and pseudoplastic liquids, *Chem Eng Sci*, **60**, 2427-2437, 2005.
 43. Cheng J, Carreau PJ, Chhabra RP, On the effect of wall and bottom clearance on mixing of viscoelastic fluids, *AIChE Symp Ser*, **91**, 115-122, 1995.
 44. Brito-de la Fuente E, Leuliet JC, Choplin L, Tanguy PA, On the effect of shear-thinning behavior on mixing with a helical ribbon impeller, *AIChE Symp Ser*, **44**, 28-32, 1992.